Supplementary Information

A multifunctional Eu-CP as Recyclable Luminescent Probe for Highly Sensitive Detection of Fe^{3+}/Fe^{2+}, $Cr_2O_7^{2-}$, and Nitroaromatic Explosives

Yang Yang, Fangzhou Qiu, Cong Xu, Yan Feng, Guolin Zhang and Weisheng Liu*

Key Laboratory of Nonferrous Metal Chemistry and Resources Utilization of Gansu Province and State Key Laboratory of Applied Organic Chemistry, College of Chemistry and Chemical Engineering, Lanzhou University, Lanzhou, 730000, China.

*Corresponding author. Tel: +86/931/8915151

Fax number: +86/931/8912582

E/mail: liuws@lzu.edu.cn

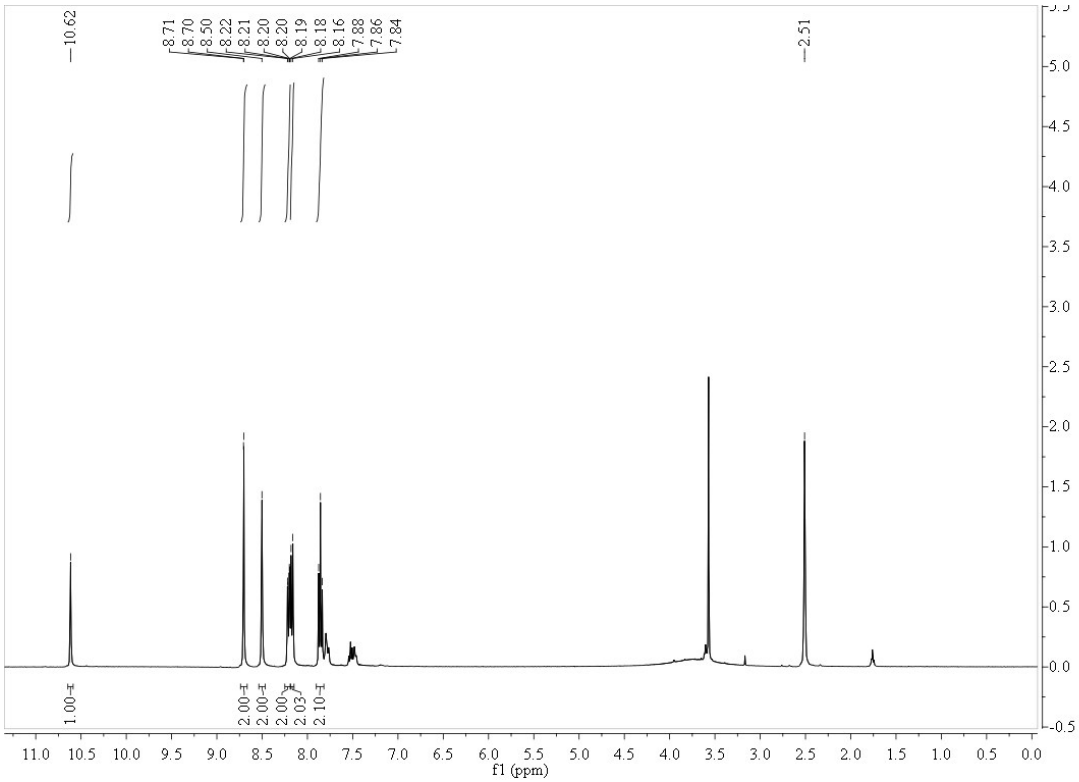

Figure S1. The ^{1}H NMR spectra of ligand L in DMSO-d_6.

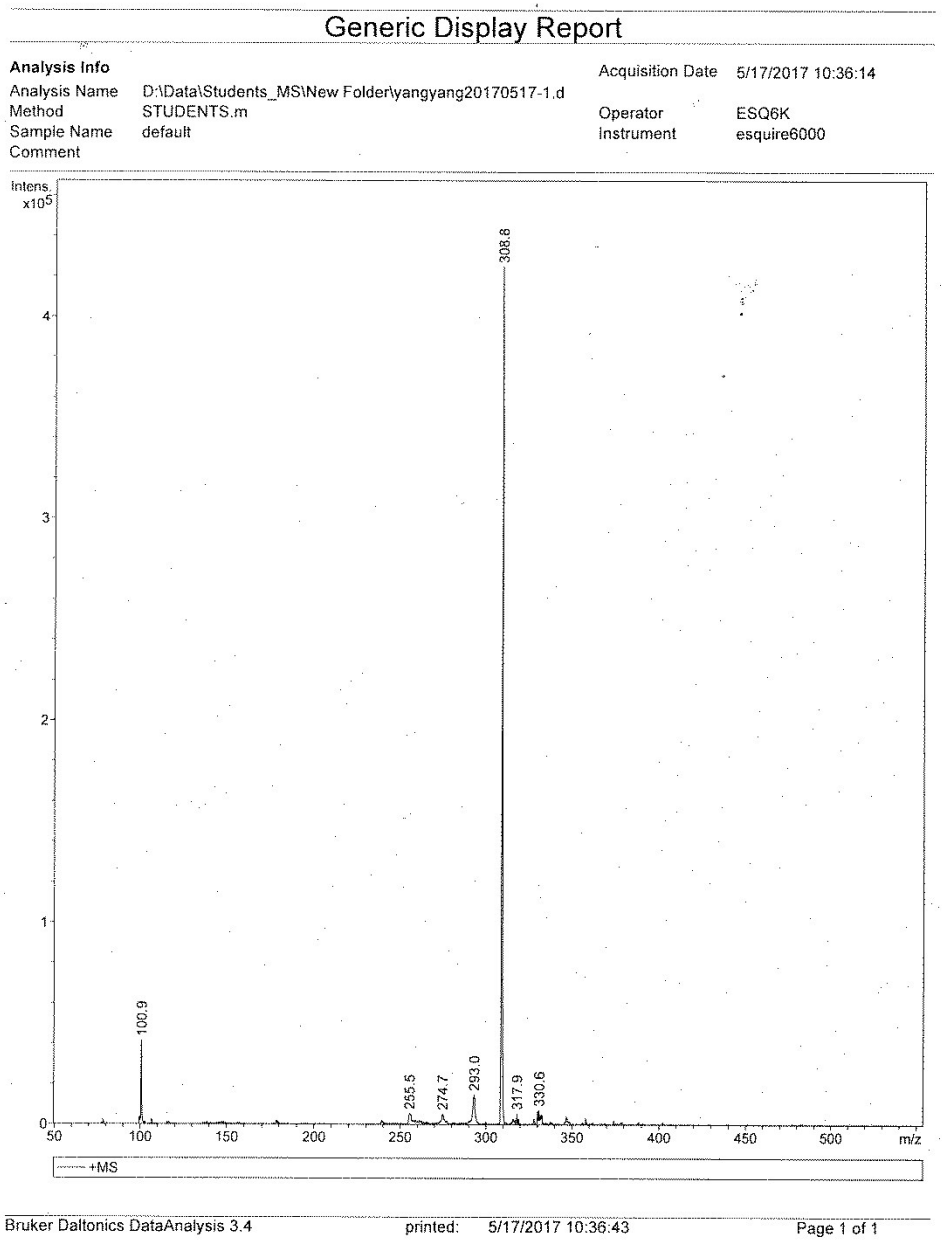

Figure S2. The Mass spectra of ligand L.

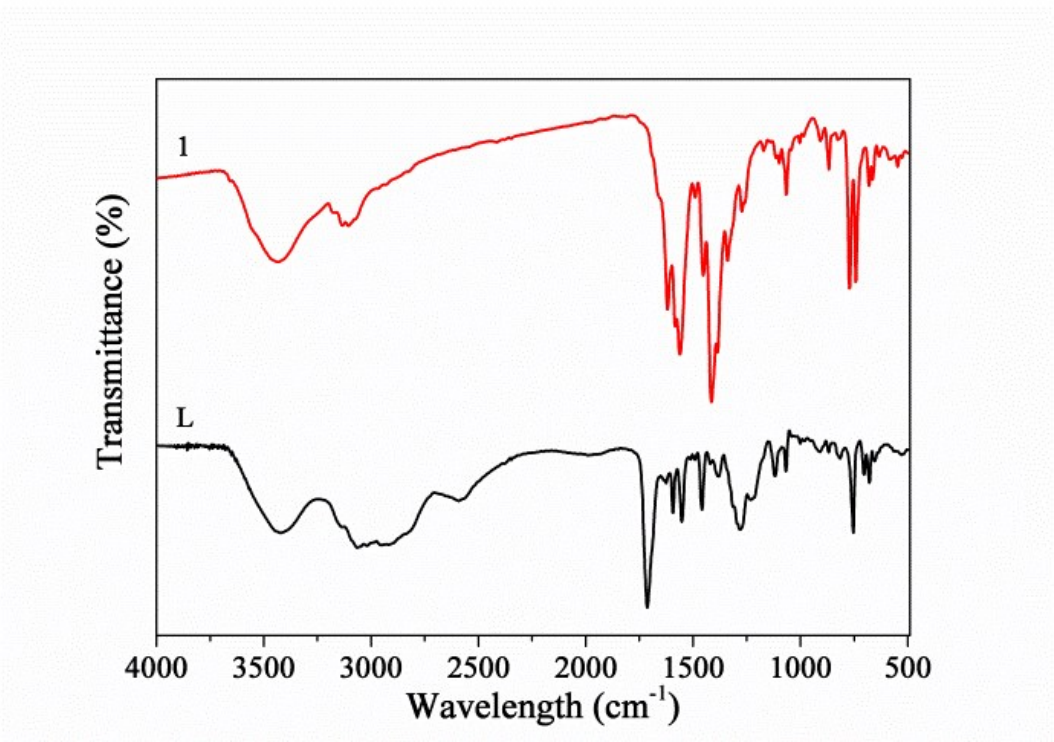

Figure S3. IR spectra of 1 and L.

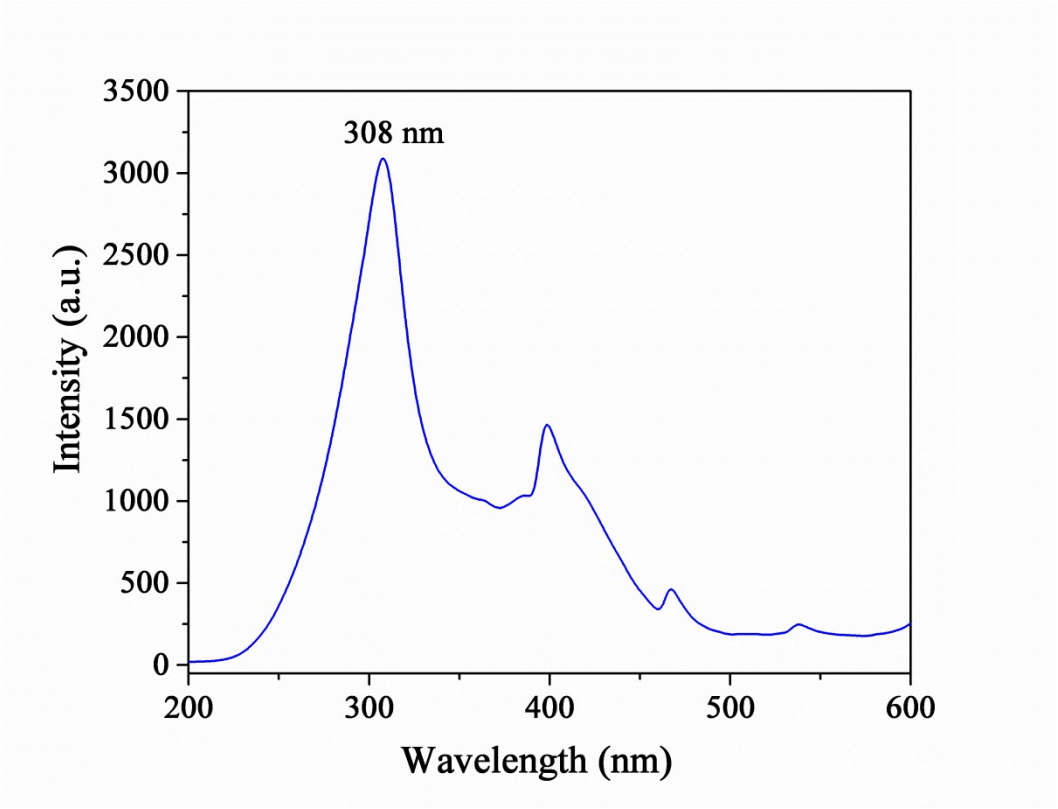

Figure S4. The excitation spectrum of **1** in CH_3CN (em = 618 nm).

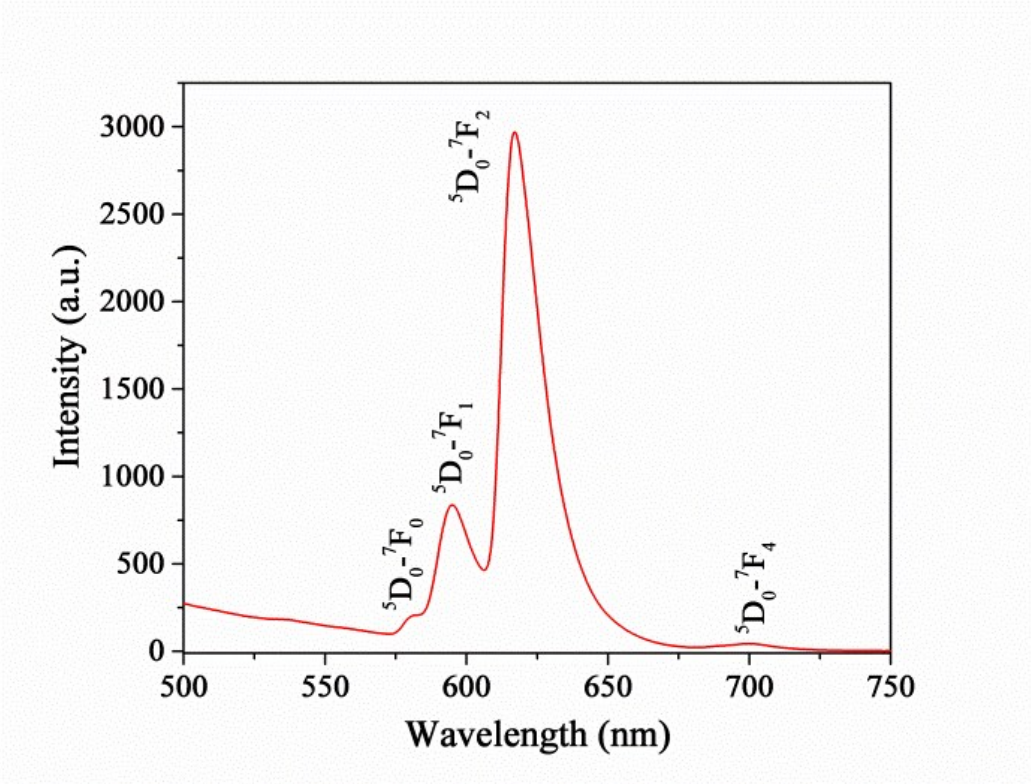

Figure S5. The emission spectrum of **1** in CH_3CN (ex = 308 nm).

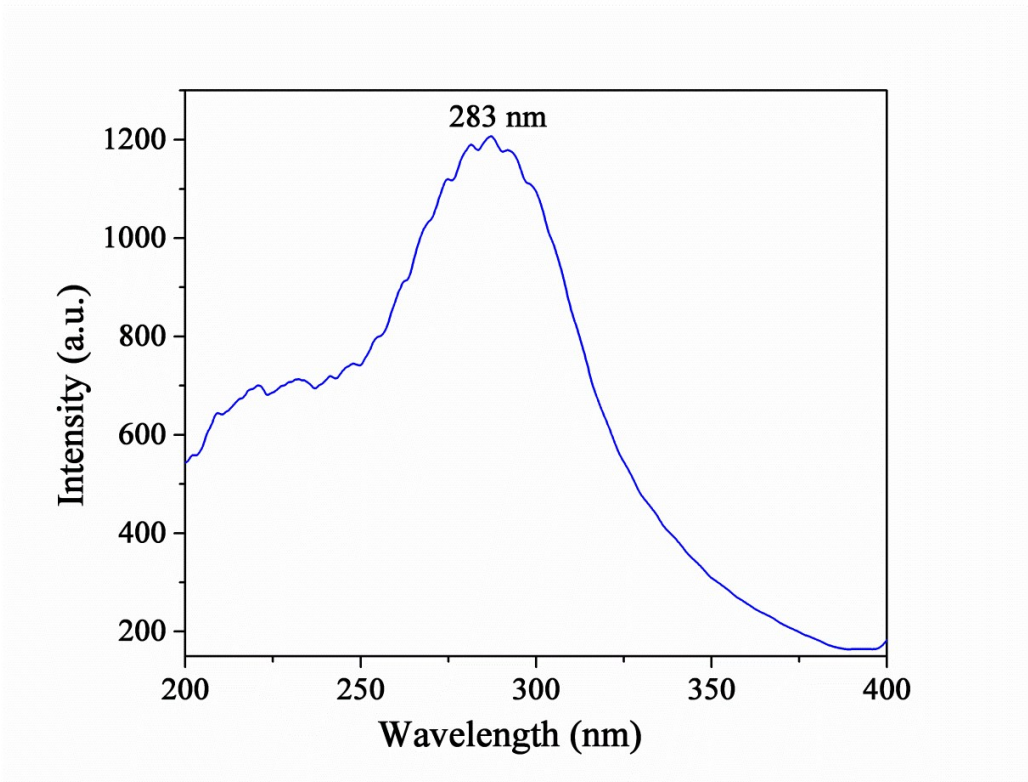

Figure S6. The solid-state excitation spectrum of **L** at room temperature (em = 415 nm).

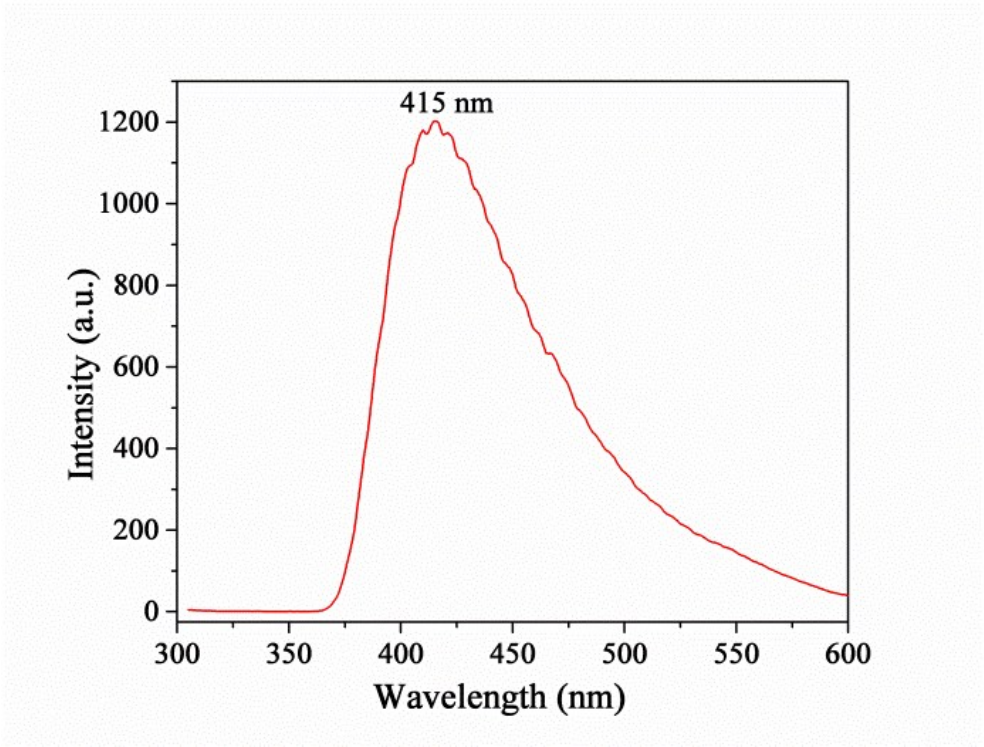

Figure S7. The solid-state emission spectrum of **L** at room temperature (ex = 283 nm).

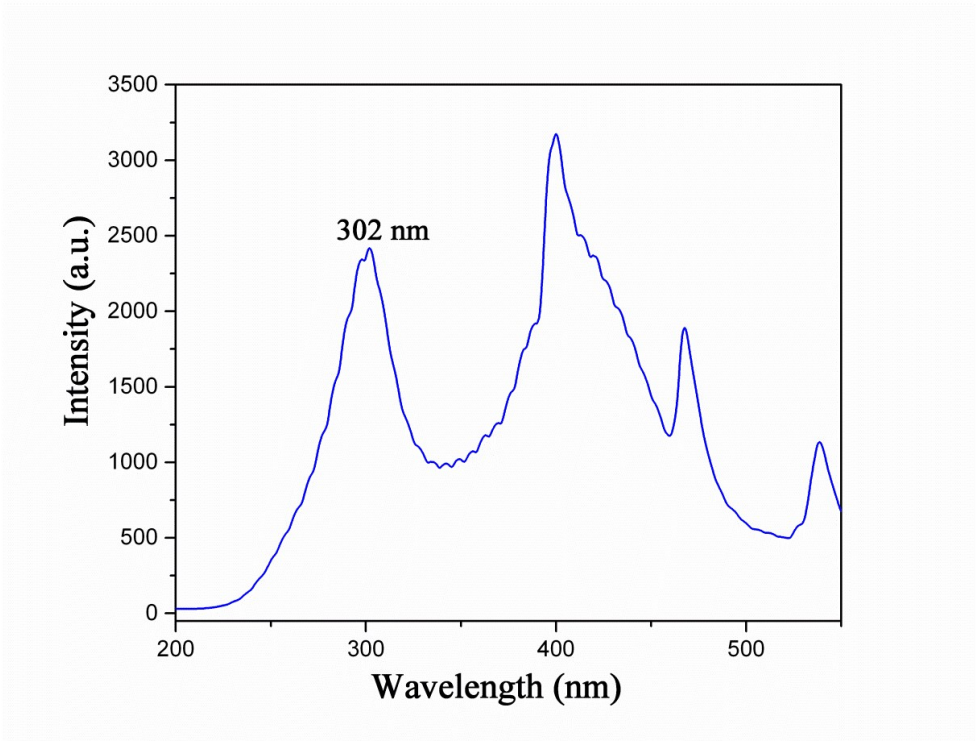

Figure S8. The solid-state excitation spectrum of **1** at room temperature (em = 617 nm)

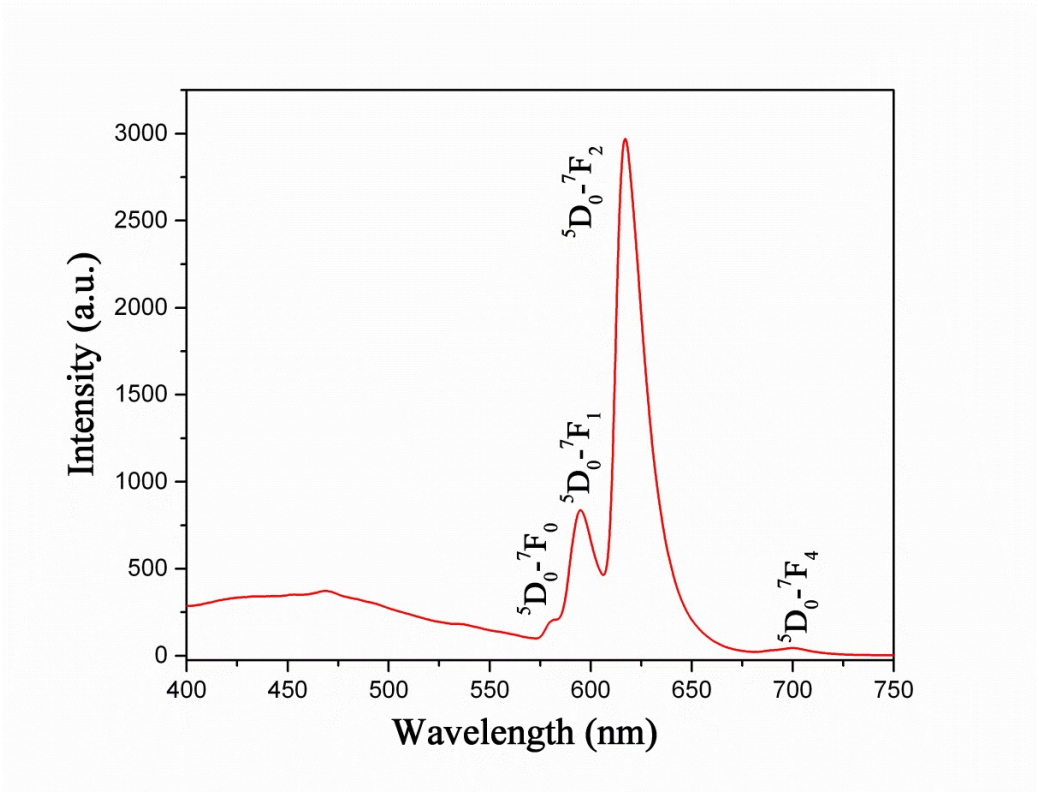

Figure S9. The solid-state emission spectrum of **1** at room temperature (ex = 302 nm).

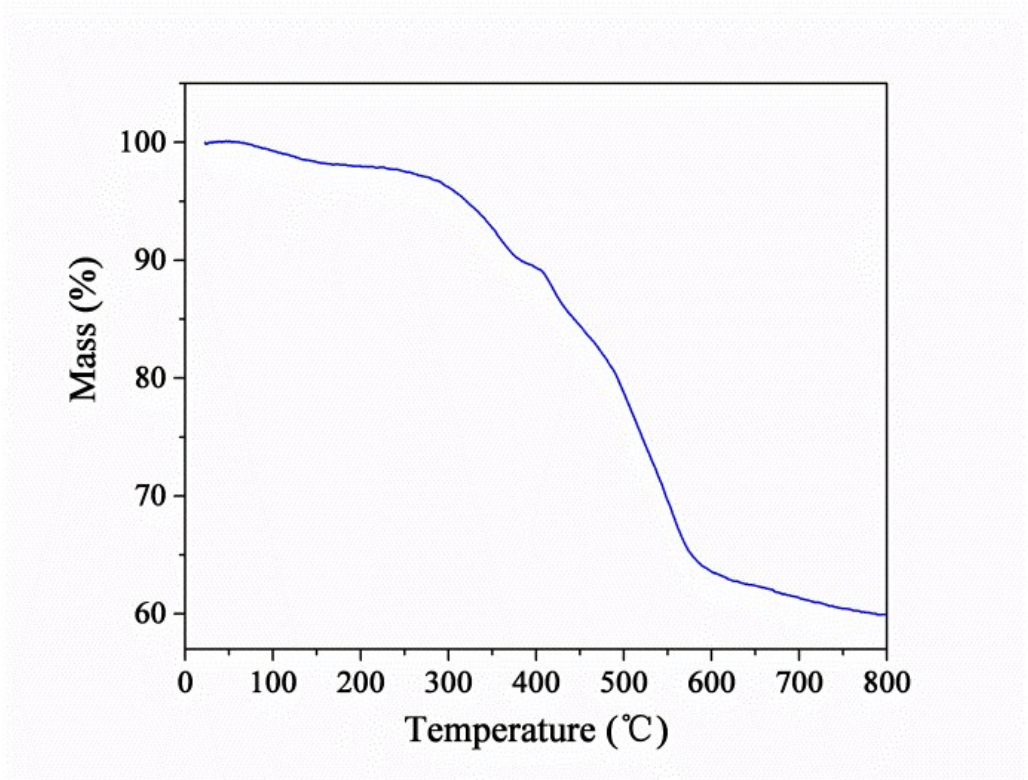

Figure S10. The TGA curves of 1.

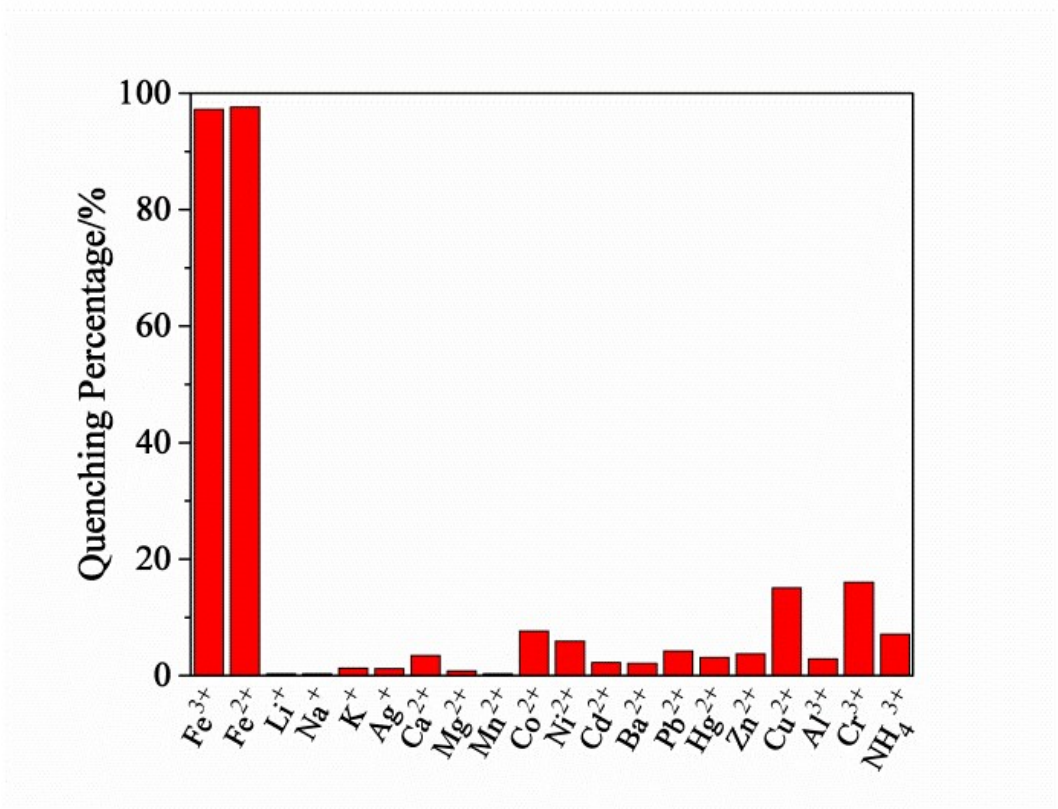

Figure S11. Luminescence quenching efficiencies of various cations towards 1 at 1 mM concentration.

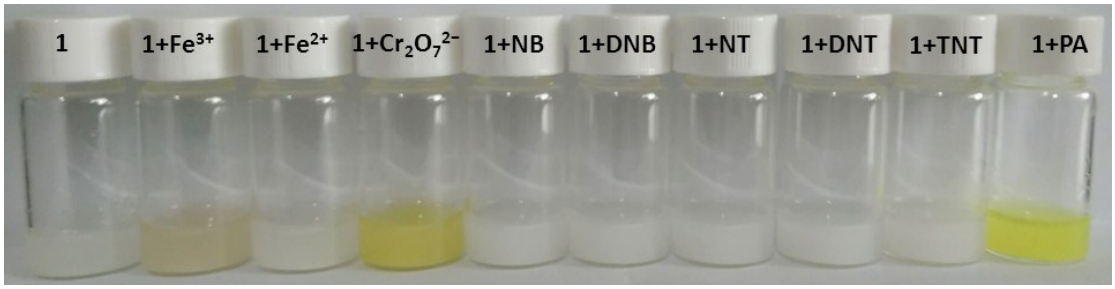

Figure S12. Color changes of 1 in the presence of various analytes.

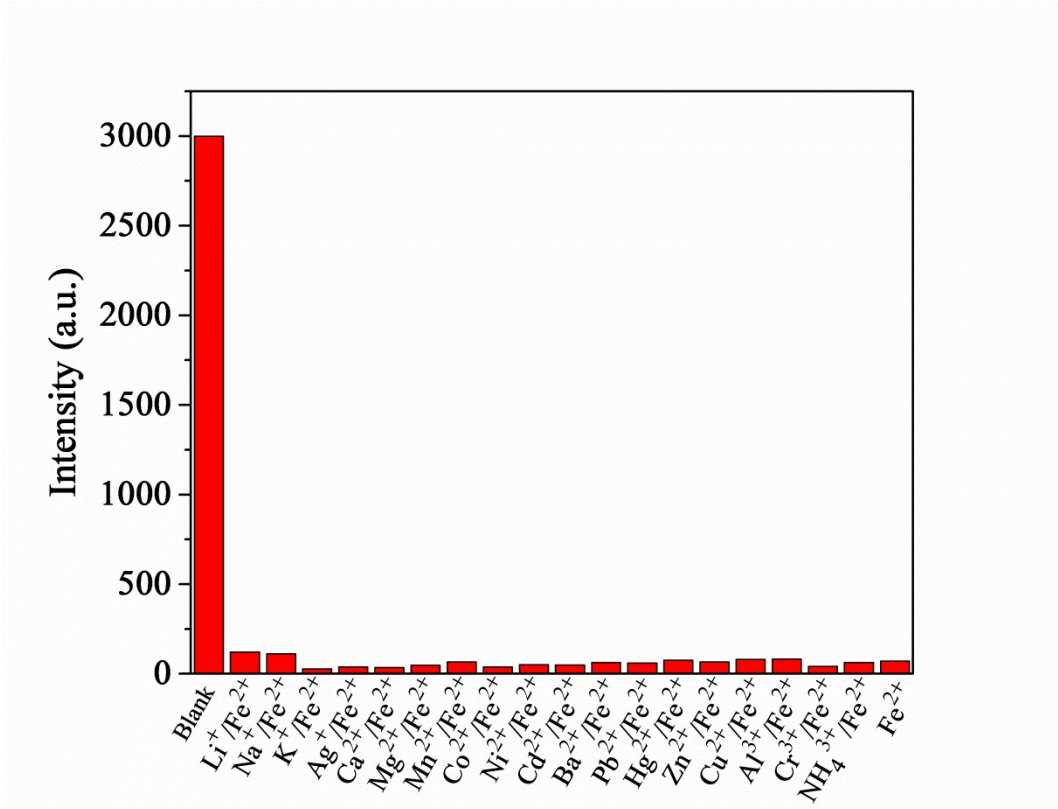

Figure S13. Luminescence intensity at 618 nm of 1 with Fe^{2+} (1×10^{-3} M) in the presence of other metal ions (1×10^{-3} M) in CH_3CN.

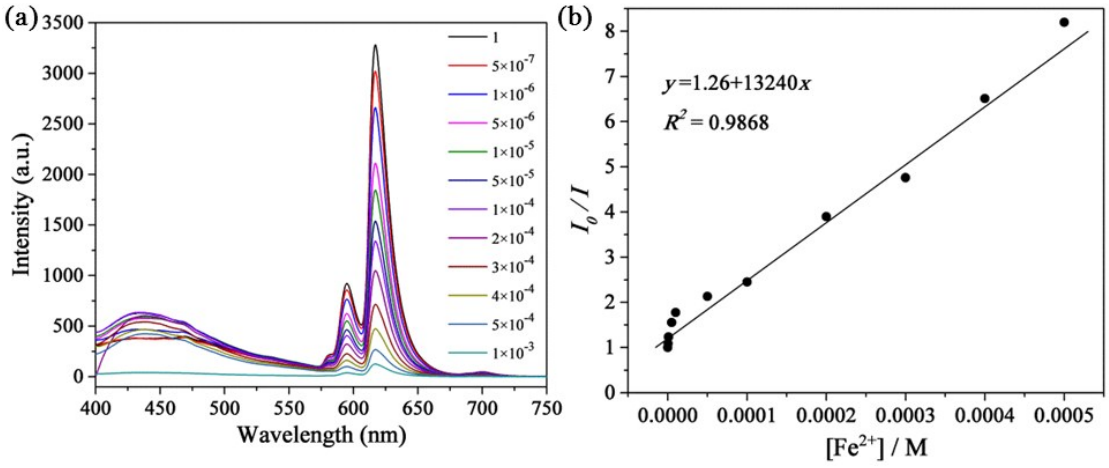

Figure S14. (a) Luminescence responses of 1 toward different concentrations of Fe^{2+} (0–1 mM) in CH_3CN (λ_{ex}= 308 nm). (b) Stern–Volmer plot of I_0/I versus increasing concentrations of Fe^{2+}.

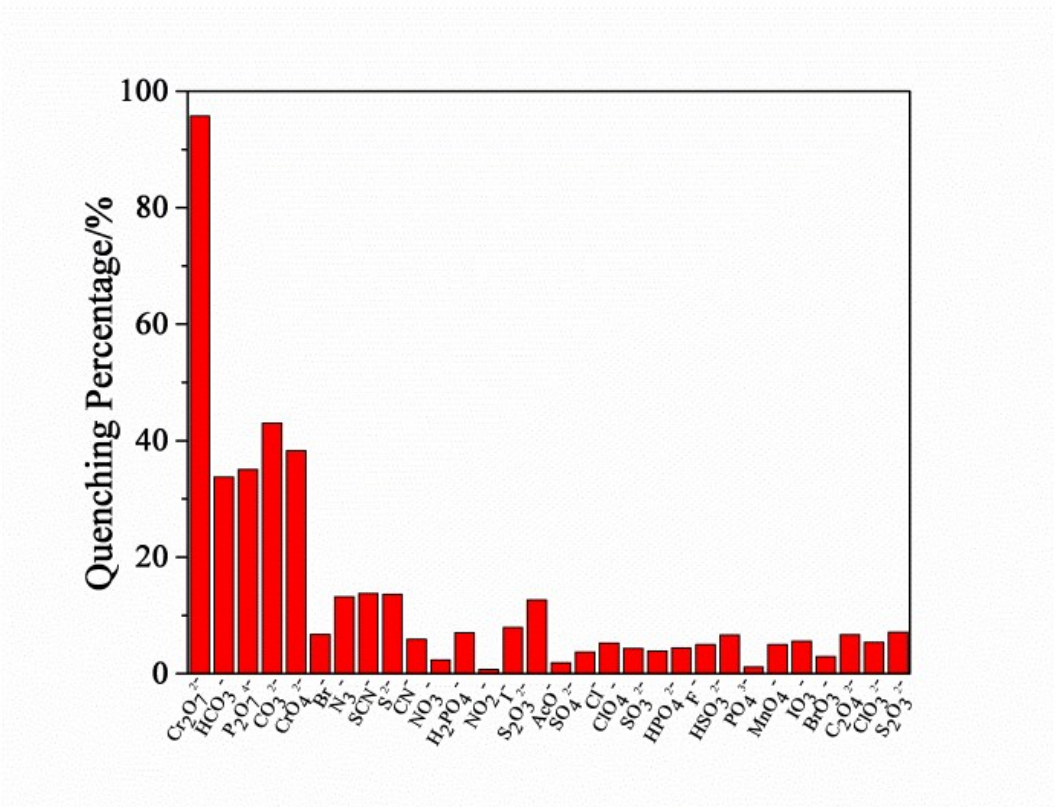

Figure S15. Luminescence quenching efficiencies of various anions towards 1 at 1 mM concentration.

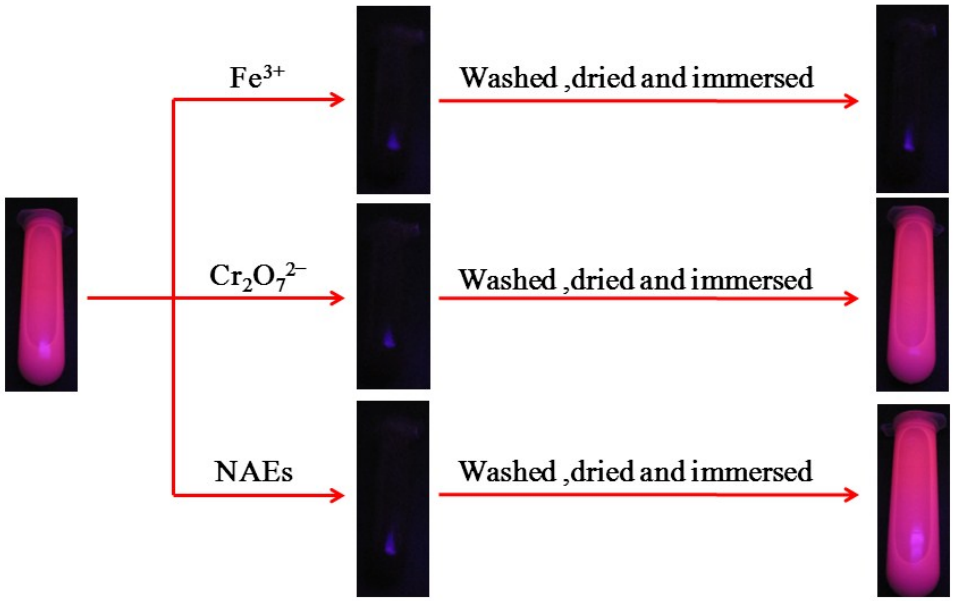

Figure S16. Optical images of 1 before and after immersion in various analytes.

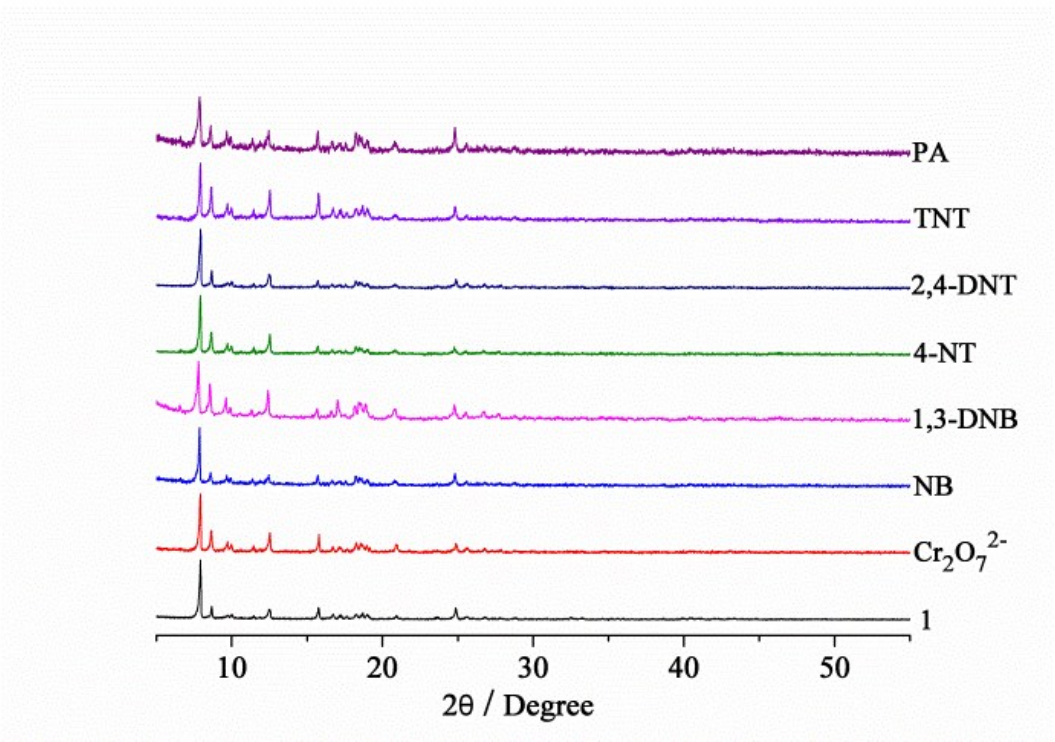

Figure S17. The PXRD patterns of **1** after five cycles experiment for the detection of various analytes.

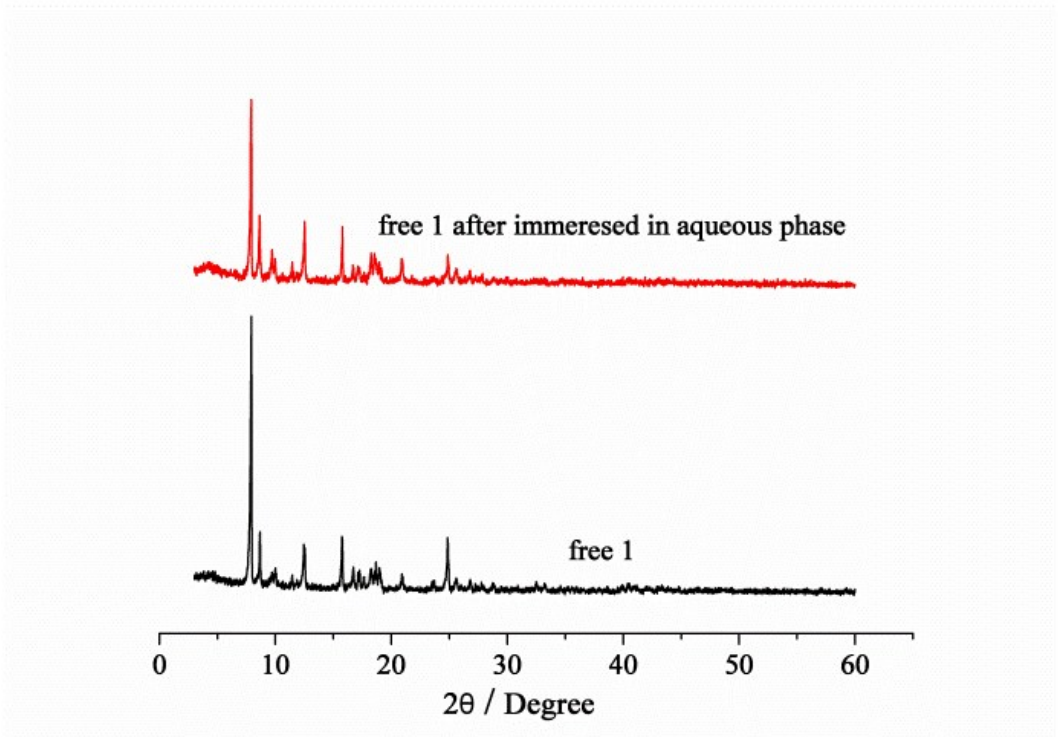

Figure S18. The PXRD patterns of **1** after immersing in aqueous solution 12 h.

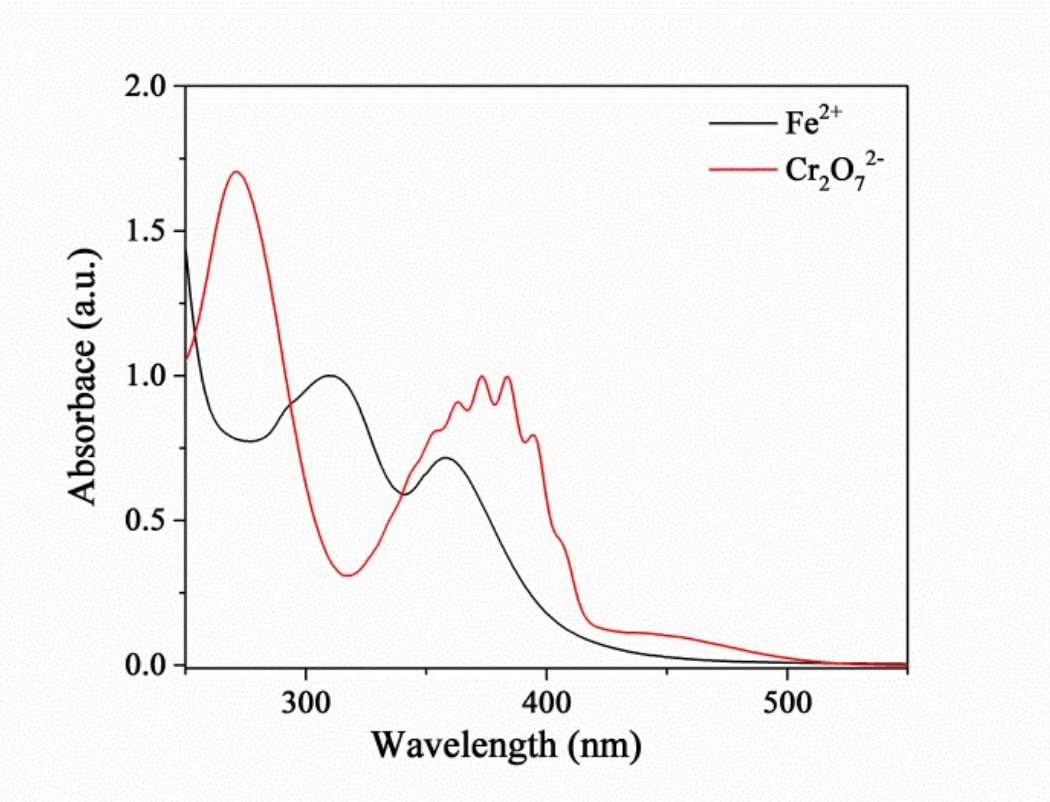

Figure S19. Absorbance spectra of Fe^{2+} and $Cr_2O_7^{2-}$ in CH_3CN.

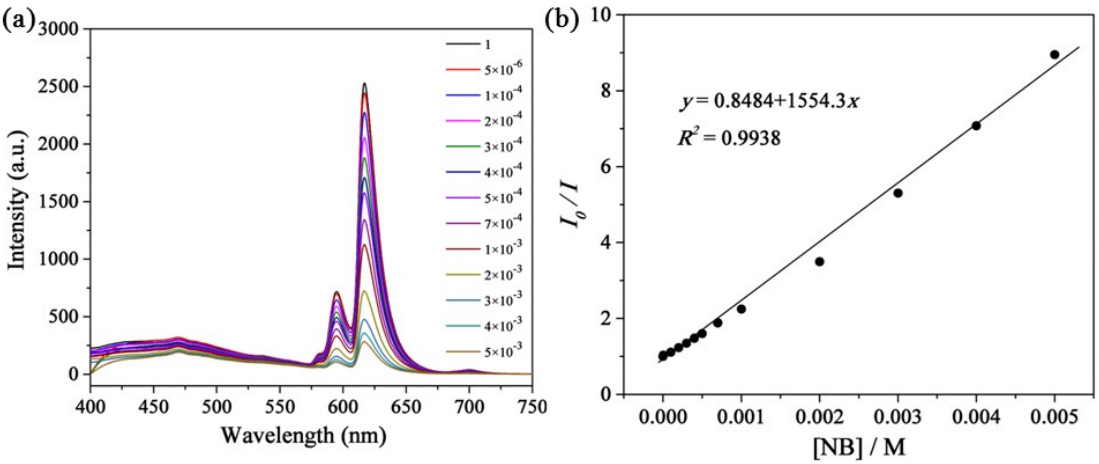

Figure S20. (a) Luminescence responses of 1 toward different concentrations of NB (0–5 mM) in CH_3CN (λ_{ex}= 308 nm). (b) Stern–Volmer plot of I_0/I versus increasing concentrations of NB.

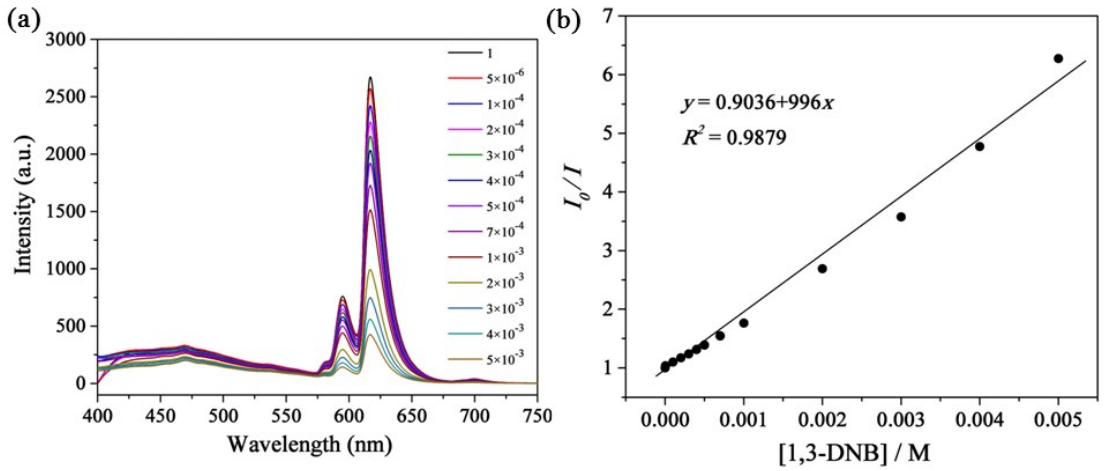

Figure S21. (a) Luminescence responses of 1 toward different concentrations of 1,3-DNB (0–5 mM) in CH_3CN (λ_{ex}= 308 nm). (b) Stern–Volmer plot of I_0/I versus increasing concentrations of 1,3-DNB.

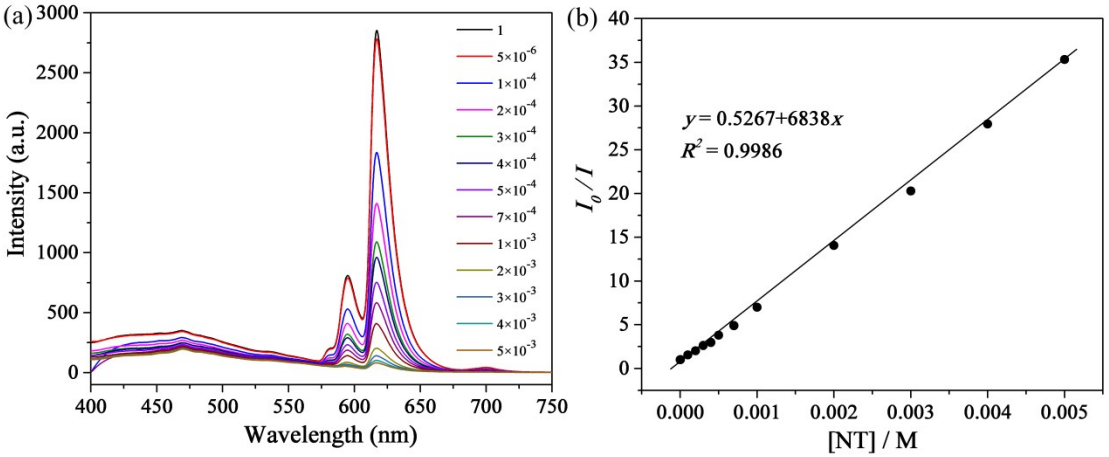

Figure S22. (a) Luminescence responses of 1 toward different concentrations of 4-NT (0–5 mM) in CH_3CN (λ_{ex}= 308 nm). (b) Stern–Volmer plot of I_0/I versus increasing concentrations of 4-NT.

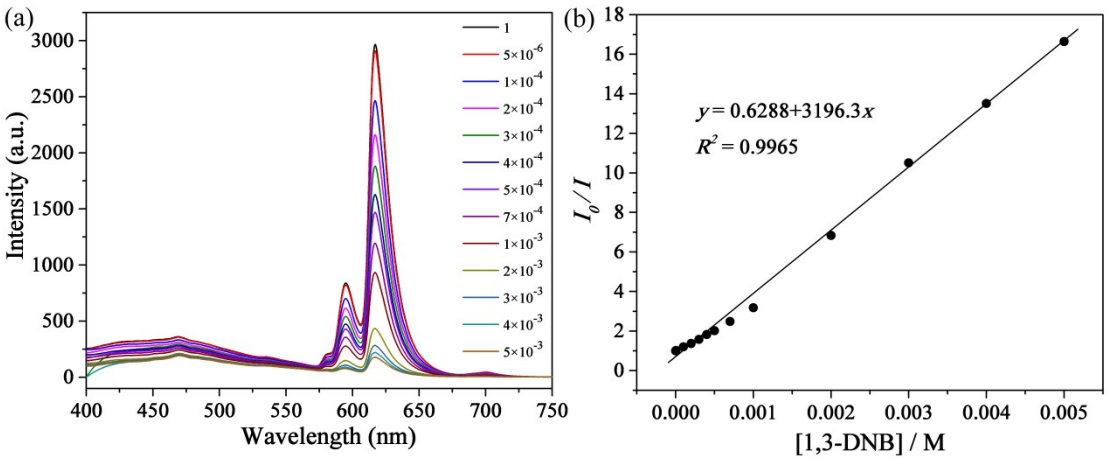

Figure S23. (a) Luminescence responses of 1 toward different concentrations of 2,4-DNT (0–5 mM) in CH_3CN (λ_{ex}= 308 nm). (b) Stern–Volmer plot of I_0/I versus increasing concentrations of 2,4-DNT.

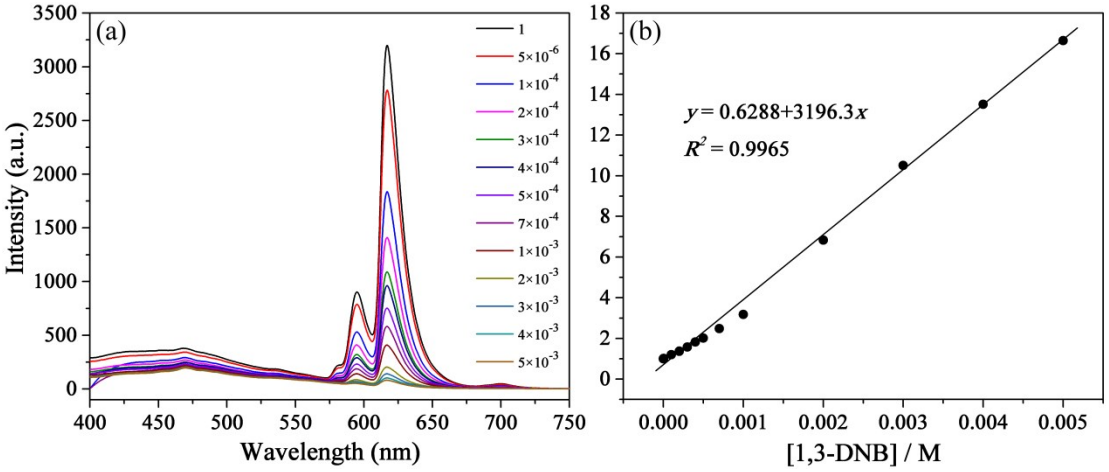

Figure S24. (a) Luminescence responses of 1 toward different concentrations of TNT (0–5 mM) in CH_3CN (λ_{ex}= 308 nm). (b) Stern–Volmer plot of I_0/I versus increasing concentrations of TNT.

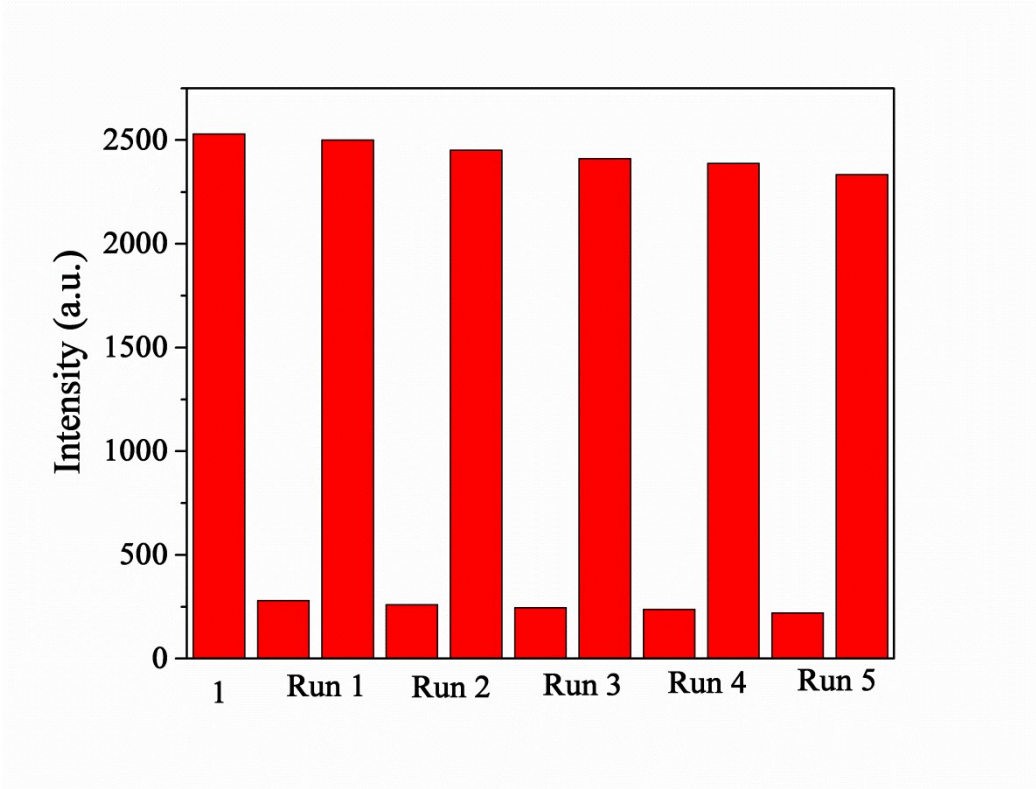

Figure S25. Repeatability of the quenching ability of 1 in CH_3CN and in the presence of NB (5 mM) (λ_{ex} =308 nm).

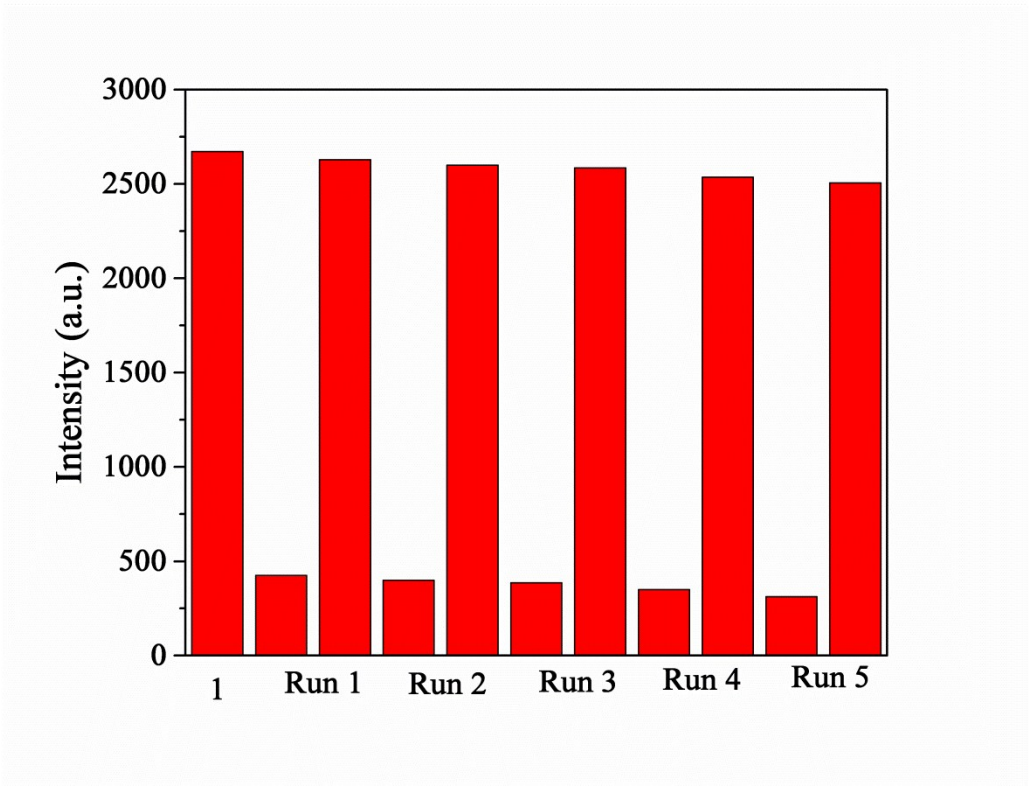

Figure S26. Repeatability of the quenching ability of 1 in CH_3CN and in the presence of 1,3-DNB (5 mM) (λ_{ex} =308 nm).

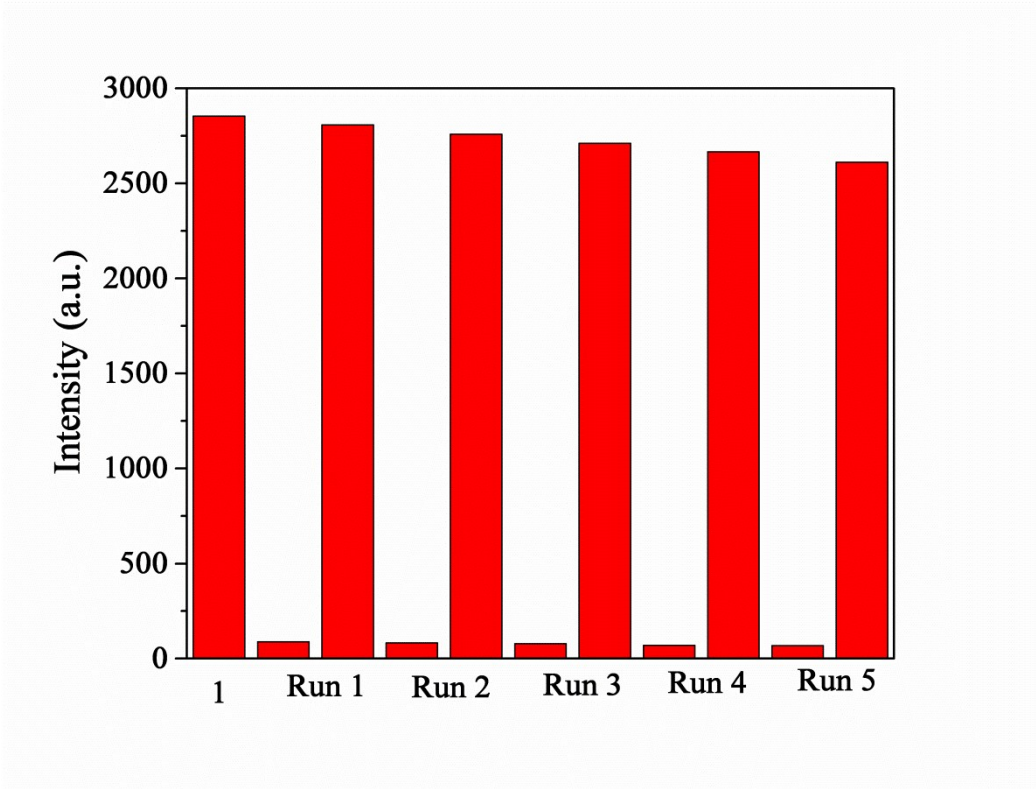

Figure S27. Repeatability of the quenching ability of 1 in CH_3CN and in the presence of 4-NT (5 mM) (λ_{ex} =308 nm).

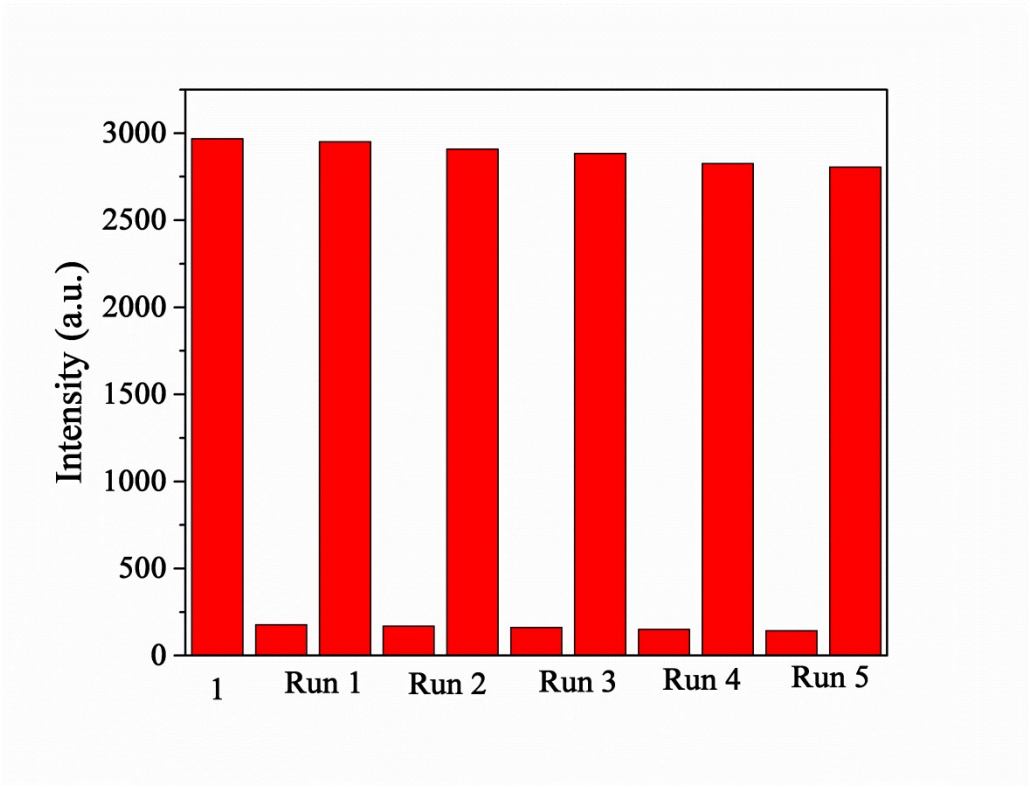

Figure S28. Repeatability of the quenching ability of 1 in CH_3CN and in the presence of 2,4-DNT (5 mM) (λ_{ex} =308 nm).

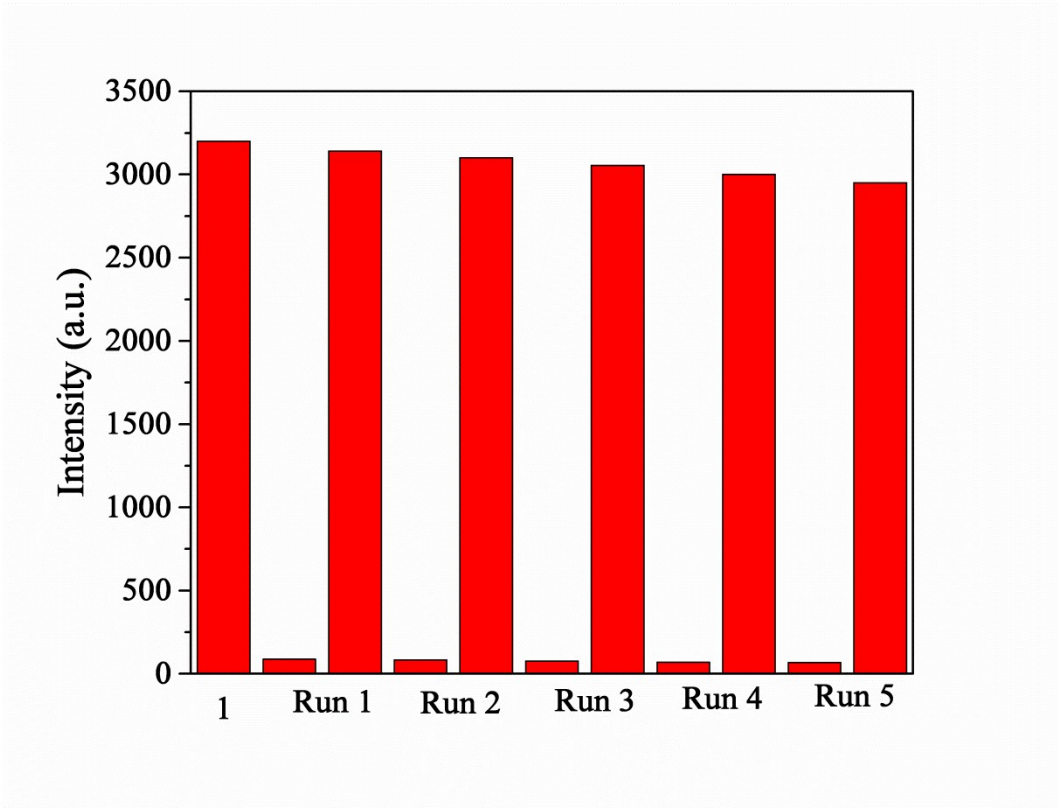

Figure S29. Repeatability of the quenching ability of 1 in CH_3CN and in the presence of TNT (5 mM) (λ_{ex} =308 nm).

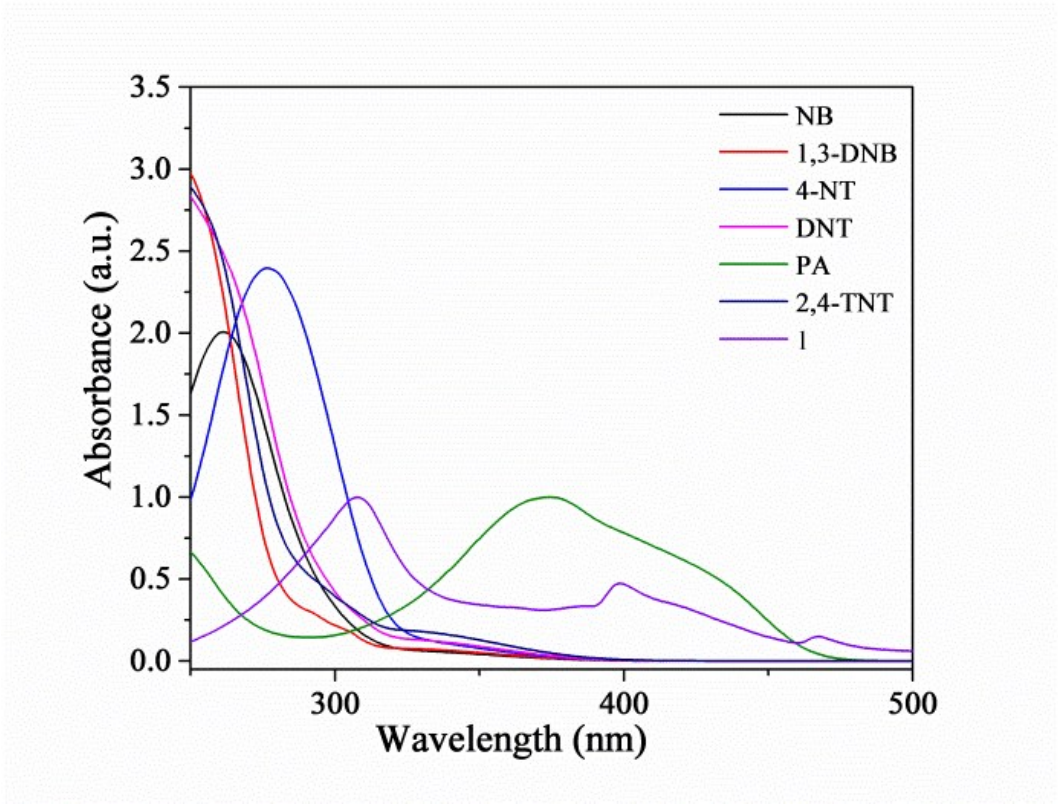

Figure S30. The absorbance spectra of various NAEs in CH_3CN.

Table S1. Crystal data and structure refinement for 1**.**

Compound	1
Empirical formula	$C_{34}H_{22}EuN_5O_{11}$
Formula weight	828.52
Crystal system	triclinic
Space group	P—1
a/Å	10.5851(11)
b/Å	11.3157(11)
c/Å	13.7776(10)
α/°	92.788(7)
β/°	101.970(8)
γ/°	92.107(8)
Volume/Å^3	1610.6(3)
Z	2
D_{calc} g/cm^3	1.709
μ/mm^{-1}	1.997
F(000)	824.0
Crystal size/mm^3	0.31×0.25×0.2
Reflections collected	12315
Independent reflections	5174
Data/restraints/parameters	6290/42/460
Goodness-of-fit on F^2	1.08
Final R indexes [I>=2σ (I)]	R_1= 0.0559, wR_2= 0.1285
Final R indexes [all data]	R_1= 0.0716, wR_2= 0.1431